31st International Conference
ENGINEERING MECHANICS 2025
Medlov, Czech Republic, May 12 –14, 2025
Paper #6, pp. 49–52, doi: 10.21495/em2025-49

EXPERIMENTAL INVESTIGATION INTO WHIRL FLUTTER USING W-WING AEROELASTIC DEMONSTRATOR IN 2024

Čečrdle J.[1], Malínek P.[2], Vích O.[3]

Abstract: *This paper discusses the recent accomplishments in the testing of the W-WING whirl flutter demonstrator. First, the paper gives a theoretical background on the whirl flutter phenomenon and outlines information about the demonstrator itself, past design and development activities and preparatory experiments including mass and stiffness measurements, modal tests and engine tests. The main focus is paid on the wind tunnel measurements. The wind tunnel test description includes the test equipment and methodology as well as the test result assessment methodology and examples of the results. Finally, the outcome and future activities are outlined.*

Keywords: Flutter, Whirl flutter, W-WING, OFELIA project

1. Introduction

Whirl flutter is a specific type of aeroelastic flutter instability, discovered by Taylor and Browne (1938). It may appear on turboprop aircraft due to the effect of rotating parts, such as a propeller or a gas turbine engine rotor. The complicated physical principle of whirl flutter requires experimental validation of the analytical results. In particular, the analytical solution of the propeller aerodynamic forces is unreliable. Further, structural damping is a key parameter, to which whirl flutter is extremely sensitive and which needs to be validated. Therefore, aeroelastic models are used. A comprehensive exposition on whirl flutter experimental research is provided by Čečrdle (2023). VZLU's previous experimental activities included aeroelastic wind tunnel testing in the frame of the Czech aircraft structures certification. Aeroelastic models of aircraft structures are currently utilized as research demonstrators for research of novel concepts, systems, methods, etc. The subjected W-WING research demonstrator represents the half-wing and engine with a powered rotating propeller of a typical commuter turboprop aircraft structure.

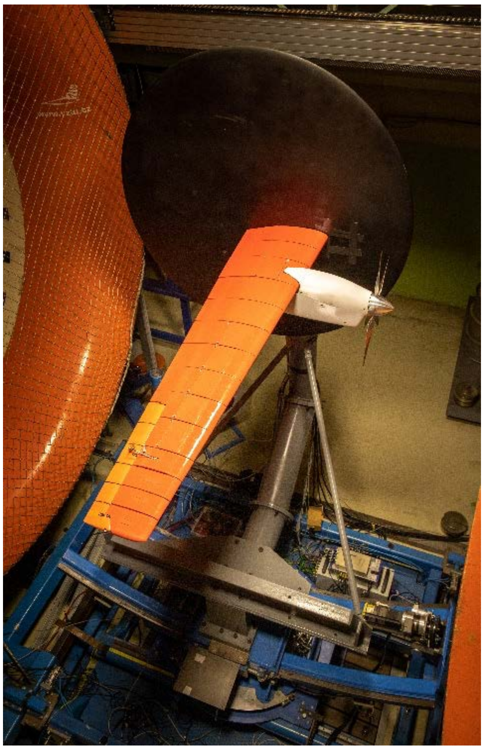

Fig. 1: W-WING research demonstrator

2. W-WING Whirl Flutter Aeroelastic Demonstrator

Whirl flutter aeroelastic demonstrator (W-WING) was adapted from a half-wing with a span of 2.56 m with the engine of a former aeroelastic model of the commuter aircraft for 40 passengers. The total mass of the model is approximately 55 kg. The wing and aileron stiffness is modeled by a duralumin spar of variable cross-section. The inertia characteristics are modeled by lead weights. The aileron is actuated by the

[1] Ing. Jiří Čečrdle, Ph.D.: Czech Aerospace Research Centre (VZLU), Beranových 130; 199 05, Prague; CZ, cecrdle@vzlu.cz
[2] Ing. Petr Malínek: Czech Aerospace Research Centre (VZLU), Beranových 130; 199 05, Prague; CZ, malinek@vzlu.cz
[3] Ing. Ondřej Vích: Czech Aerospace Research Centre (VZLU), Beranových 130; 199 05, Prague; CZ, ondrej.vich@vzlu.cz

electromagnetic shaker placed at the wing root via a push-pull rod. The nacelle model has two DOFs (engine pitch and yaw). The stiffness parameters are modeled by means of cross-spring pivots. The leaf springs are changeable, and the stiffness parameters can be adjusted independently by replacing the spring leaves. Both pivots are independently movable in the direction of the propeller axis to adjust the pivot points of both vibration modes. The inertia of the engine is modeled by the replaceable and movable weight. The gyroscopic effect of the rotating mass is simulated by the mass of the propeller blades. The propeller is powered by an electric motor with a nominal power of 15 kW. This power enables to provide the measurement in thrusted propeller conditions. The demonstrator in the wind tunnel test section is shown in figure 1. Motor is equipped with servo-amplifier to manage and evaluate propeller revolutions, torque, and immediate power. In addition, an independent rpm sensor is installed. Finally, a balance cell for the measurement of the propeller thrust is installed. Demonstrator is equipped with a system of aerodynamic excitation by aileron flapping deflection. Aileron is actuated via push-pull rod using an electromagnetic shaker (and amplifier) placed behind the splitter plate.

Fig. 2: Complete model modal test arrangement.

Mechanical instrumentation includes strain gauges in the root and half-span sections to measure the vertical bending, in-plane bending, and torsional deformations of the wing. Demonstrator is also equipped with 18 uniaxial accelerometers. Wing is instrumented at six spanwise sections and two positions chordwise for the vertical direction and at a single position in the wingtip for the in-plane (longitudinal) direction. Nacelle is instrumented in two sections (front and rear) for both vertical and horizontal directions and at the rear section also for the longitudinal direction. The data acquisition and processing are provided using in-house LabVIEW-based application. The application is also used to control the propeller rotation and to manage the aerodynamic excitation by the aileron flapping. Finally, the application provides a safeguard preventing the destruction of the demonstrator, provided the response at the critical points exceeds the preset threshold. The data are acquired with the sampling frequency of 2000 Hz and depicted in the time domain as well as pre-processed into the form of power spectral densities. Apart from the described application, the LMS TestLab system is used. The system acquires continuous signals from all accelerometers and the airflow velocity signal. The amplitude evolution of the frequency components corresponding to the engine whirl motion are monitored in real-time. The data are then used for the assessment of the demonstrator's vibration response using the methods of FFT and OMA.

Fig. 3: Complete model OMA, configuration with propeller substitute disc.

3.Ground Tests

Ground tests were aimed at determining the static and dynamic characteristics of the demonstrator and the operational limits of the power system. First, the

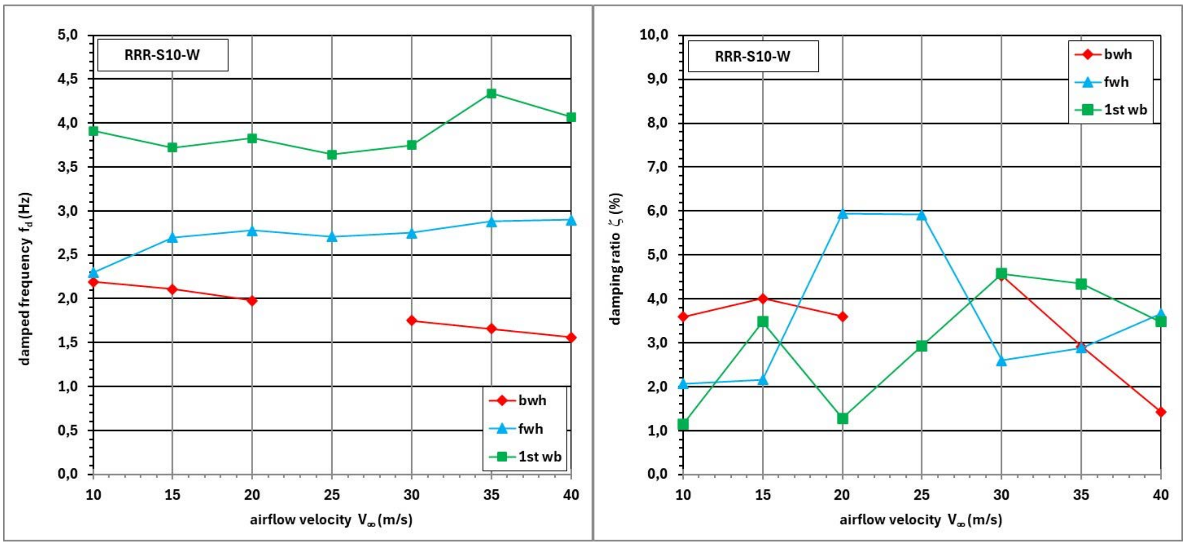

Fig. 4: Example of results, V-f diagram (a) and V-g diagram (b), backward whirl, forward whirl and 1st wing bending modes

nacelle component tests were performed. These tests included stiffness tests to obtain effective stiffness in pitch and yaw directions and modal tests to obtain engine pitch and yaw frequencies. These tests included all five variants of cross spring pivot leaves thickness. Next, the complete model modal tests to obtain modal characteristics of the complete model, i.e., including the wing modes was performed for a single configuration. Complete model modal test arrangement is shown in figure 2. Further, the operational modal analysis (OMA) was performed for the same configuration. OMA was performed in the conditions of the rotating propeller at 1000, 2000 and 3000 rpm with the angle of attack of 5, 10 and 15 degrees. In addition, the measurement using the mass equivalent disc was performed (figure 3). The purpose was to describe the effect of the propeller rotation onto modal parameters and to split the effect of aerodynamic and dynamic forces. Finally, the power plant operation tests were performed to find the maximal available revolutions for various angles of attack with respect to the available power.

4. Wind Tunnel Test

The demonstrator is designed for testing in the VZLU 3-m diameter low speed wind tunnel. The demonstrator, combined with the splitter plate which prevents the induced effects at the wing root region, is fixed to the attachment arm inside the wind tunnel test section as shown in figure 1. The measurement variant was defined by these structural parameters: pitch and yaw attachment stiffness, pitch and yaw hinge station, balance weight station, choice of propeller (duralumin or steel blades), and finally, by the propeller blade 75% section angle of attack (α). First, the measurement of the pitch and yaw frequencies without the airflow was performed because the pitch and yaw effective stiffness is influenced also by the conditions of assembly. Next, the main measurement including airflow was performed. In the first phase, the excitation

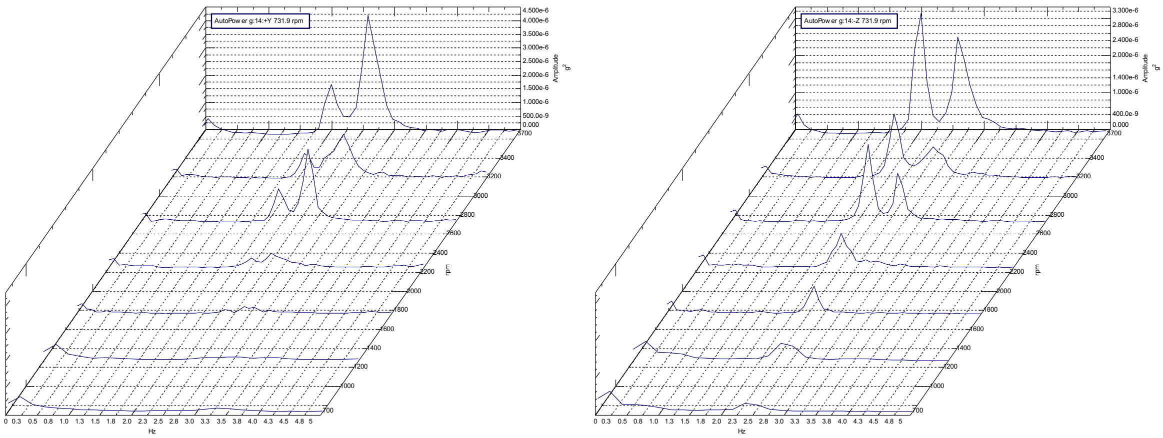

Fig. 5: Example of results, power spectra.

was realized by the flow turbulence only. Next the measurement was repeated with the excitation by the aileron harmonic sweep flapping. The duration of measurement at a single velocity was approximately 1 minute, after steady propeller revolutions were reached.

Measured variants include a single choice of the yaw and pitch stiffness (V2), two choices of the yaw and pitch pivot station (front and rear), two choices of the weight station (front and rear), two choices of the propeller (duralumin and steel), two choices of the blade angle of attack (5 and 10 deg.) and four choices of the propeller RPM (windmilling, 3600, 4000 and 4400). All variants were tested with the excitation by the airflow turbulence and by the aileron flapping. Thus, 128 measurement runs were performed in total.

Vibration records were processed using FFT. The spectra were sorted by the time and displayed as cascade graphs in the broad frequency range. The airflow velocity waveform is also important. Propeller revolutions, airflow velocity and the vibration spectra at the measured points provide global information on the dynamic behavior of the structure at a certain time. A detailed assessment in the frequency domain was focused on the frequency range from 0 to 20 Hz. Further, the averaged Cross Power and Auto Power spectra of vibrations were evaluated at the measured points. The data of the runs with the turbulence excitation were the input in the OP Time MDOF algorithm for the operational modal analysis (OMA). The results include modal parameters (frequency, mode shape, damping ratio) of the evaluated modes at the particular airflow velocities ranging from 10 to 40 m/s. The identified modes include both backward and forward whirl modes as well as the wing modes, especially 1st bending mode. The example diagrams velocity – frequency – damping are presented in figure 4. It can be observed that there is a decrease in the frequency of the backward whirl mode while the forward whirl mode shows an increase in frequency with the airflow velocity. Similar can be observed also from the example of the power spectra presented in figure 5. Secondary results include the propeller windmilling rpm, propeller thrust and immediate power. The example presented in figure 6 represents the propeller thrust at 4400 rpm.

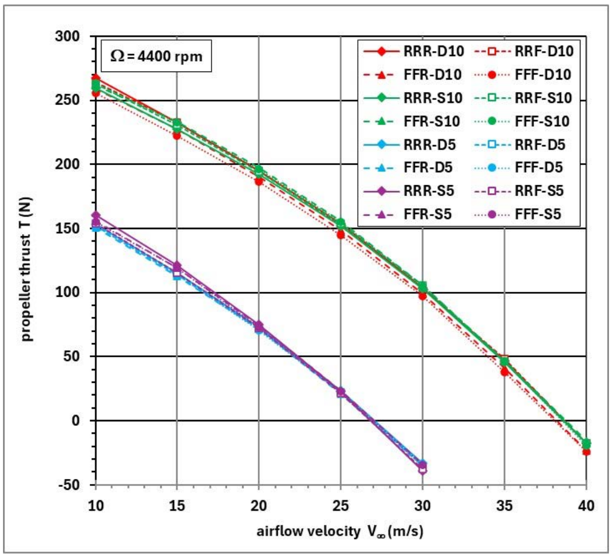

Fig. 6: Propeller thrust, RPM = 4400.

5. Conclusion and Outlook

The paper describes the recent accomplishments in the testing of the W-WING whirl flutter demonstrator. Main focus is paid on the first experimental campaign that was accomplished in the VZLU 3m-diameter low speed wind tunnel in May 2024. The next measurement planned for 2025 will include mainly the measurements in the fixed-thrust regime. In addition to the mechanical measurements of the structure vibrational response, the aerodynamic flow field measurements are planned. The experimental results will be subsequently utilized for verification of the analytical models and computational tools (Dugeai et. al. (2011)) that will be used for development of the new power plant system, characterized as an open-fan concept, utilized for a new generation short-medium range turboprop aircraft.

Acknowledgement

Program and topic: HORIZON-JU-CLEAN-AVIATION-2022-01-SMR-01, Ultra Efficient Propulsion Systems for Short and Short-Medium Range Aircraft. Project nr. and title: 101102011, Open Fan for Environmental Low Impact of Aviation (OFELIA).

References

Čečrdle, J. (2023) *Whirl Flutter of Turboprop Aircraft Structures*, 2nd ed., Elsevier Science, Oxford, UK.

Dugeai, A., Mauffrey, Y. and Sicot, F. (2011) Aeroelastic Capabilities of the elsA Solver for Rotating Machines Applications, *Proc. Int. Forum on Aeroelasticity and Structural Dynamics*, Paris, France.

Taylor, E. S. and Browne, K. A. (1938) Vibration Isolation of Aircraft Power Plants, *J. Aerosp. Sci.*, 6(2):43-49.